Polymer Chemistry

PAPER

View Article Online
View Journal | View Issue

Cite this: *Polym. Chem.*, 2015, **6**, 3290

Group 4 metal complexes bearing the aminoborane motif: origin of tandem ring-opening metathesis/vinyl-insertion polymerization†

M. Wang,[a] G. Xu,[a] D. Wang,[a] Y. Zou,[a] W. Frey[b] and M. R. Buchmeiser*[a,c]

Received 26th February 2015,
Accepted 19th March 2015

DOI: 10.1039/c5py00303b

www.rsc.org/polymers

Three tailored *ansa*-type Zr(IV)- and Hf(IV)-complexes, **Zr-1**, **Hf-1** and **Zr-2**, all bridged by a dimethylsilylene group and bearing both a 6-[2-(BR_2)phenyl]pyrid-2-yl motif (R = ethyl, mesityl) and an η^1/η^5-bound ligand with different Lewis base character and steric demand, have been synthesized. Their structures have been determined by single-crystal X-ray diffraction analysis. Upon activation with methylalumoxane (MAO), **Zr-1**, **Hf-1** and **Zr-2** are capable of polymerizing norborn-2-ene (NBE) *via* ring-opening metathesis polymerization (ROMP). In the MAO-activated copolymerization of ethylene (E) with NBE; however, pure vinyl insertion polymerization (VIP)-derived poly(NBE)-*co*-poly(E) is obtained by **Zr-1**, **Hf-1** and the model pre-catalyst (**Zr-3**), which does not contain the borylamino motif. In contrast, **Zr-2** yields copolymers containing both ROMP- and VIP-derived poly(NBE)$_{ROMP}$-*co*-poly(NBE)$_{VIP}$-*co*-poly(E) units *via* an α-H elimination process. Variable-temperature ^{11}B NMR measurements allow for identifying tri- and tetracoordinated borane species. The propensity of catalysts **Zr-1**, **Hf-1**, **Zr-2** and **Zr-3** to switch from VIP to ROMP is discussed on the basis of their structural differences. A detailed NMR study of the reaction of **Zr-1**, **Zr-2**, **Hf-1** and in particular of dimethylsilylene-bis(6-[2-(diethylboryl)phenyl]pyrid-2-ylamido)$ZrCl_2$ (**Zr-4**) with MAO and with MAO/NBE clarifies the reaction cascade from VIP to ROMP and allows for establishing a general concept for a tailored switch from VIP to ROMP within the same polymer chain, allowing for tandem VIP–ROMP copolymerization of E with NBE.

Introduction

Tailor-made pre-catalysts containing the 6-[2-(diethylboryl)-phenyl]pyrid-2-yl motif, *e.g.*, (η^5-tetramethylcyclopentadienyl)-dimethylsilylene-(6-[2-(diethylboryl)phenyl]pyrid-2-ylamido)-$TiCl_2$ or dimethylsilylene-bis(6-[2-(diethylboryl)phenyl]pyrid-2-ylamido)$ZrCl_2$, activated by methylalumoxane (MAO) are capable of forming multi-block copolymers from ethylene (E) and norborn-2-ene (NBE) with both ring-opening metathesis (ROMP)- and vinyl insertion polymerization (VIP)-derived poly-(NBE) sequences within one single polymer chain.[1–3] The structure of these unique polyolefins was confirmed by NMR; narrow polydispersity indexes (PDIs ≤ 1.3), single peaks in the GPC and the absence of glass transitions (T_g) that could be assigned to pure poly(NBE)$_{ROMP}$ further support the proposed polymer structures. These tailored cyclic olefin copolymers bear the potential for functionalization through polymer-analogous reactions at the double bonds present in the copolymers.[4–9] If successful, this approach would offer an alternative to currently investigated copolymerizations of ethylene with functional monomers such as acrylates.[10–14] In terms of polymer synthesis, the ligand system at the group 4 metals as such was designed in a way that it can switch from VIP to ROMP *via* abstraction of the α-proton from the growing polymer chain by the nitrogen at the pyrid-2-yl moiety. This proton can then in principle re-add to the metal alkylidene. The α-H elimination/addition process is controlled by the temperature-dependent dissociation propensity of the N–B bond where the boryl group and α-hydrogen at the growing polymer chain compete for the lone pair of the pyridyl group. However, apart from the 6-[2-(R_2B)phenyl]pyrid-2-ylamido]-motif, the additional structural requirements that allow for the desired tandem polymerization are not clear.[15,16] Within that

[a]*Lehrstuhl für Makromolekulare Stoffe und Faserchemie, Institut für Polymerchemie, Universität Stuttgart, Pfaffenwaldring 55, D-70569 Stuttgart, Germany. E-mail: michael.buchmeiser@ipoc.uni-stuttgart.de; Fax: +49 (0)-711-685-64050*
[b]*Institut für Organische Chemie, Universität Stuttgart, Pfaffenwaldring 55, D-70569 Stuttgart, Germany*
[c]*Institut für Textilchemie und Chemiefasern (ITCF) Denkendorf, Körschtalstr. 26, D-73770 Denkendorf, Germany*

† Electronic supplementary information (ESI) available: Single crystal X-ray structures of compounds **3** and **4**, ^{1}H-, ^{13}C-, ^{11}B-NMR spectra, temperature-dependent NMR measurements, NMR spectra of catalysts and polymers, details of single crystal X-ray analysis of **Zr-1**, **Zr-2** and **Hf-1**. CCDC 1050437, 1050441, 1050440, 1050434 and 1050442. For ESI and crystallographic data in CIF or other electronic format see DOI: 10.1039/c5py00303b

context, it also appears desirable to tailor the dissociation temperature of the N–B bond, which is ~60 °C for dimethylsilylene-bis(6-[2-(diethylboryl)phenyl]pyrid-2-ylamido)$ZrCl_2$ (**Zr-4**).[3] This can be achieved, *e.g.* either by increasing the sterics or the electron density at the boron. Since fluorenyl ligands are less Lewis basic compared to their cyclopentadienyl or tetramethylcyclopentadienyl counterparts, fluorenyl-based metal complexes bear the potential of increasing the electrophilicity of the metal and thus enhance polymerization activity.[17–20] In addition, introduction of the bulky fluorenyl moiety is known to have an effect on the stereoselectivity of the polymers produced.[20–22]

Based on these considerations, group 4 metal complexes containing the 6-[2-(diethylboryl)phenyl]pyrid-2-yl or the 6-[2-(dimesitylboryl)phenyl]pyrid-2-yl motif and a fluorenyl or tetramethylcyclopentadienyl ligand, all bridged by a dimethylsilylene group, were prepared in order to examine the polymerization behavior of the modified catalysts for potentially new polymer structures and to clarify the mechanism of the switch from VIP to ROMP.

Results

Synthesis of pre-catalysts Zr-1 and Hf-1

6-[2-(Diethylboryl)phenyl]pyridine-2-amine (**1**)[2,3] and 9-(chlorodimethylsilyl)-9*H*-fluorene (**2**)[23–25] were prepared as described in the literature. The synthetic routes to **Zr-1** and **Hf-1** are shown in Scheme 1. Deprotonation of **1** by *n*-butyllithium (*n*-BuLi) in diethyl ether followed by reaction with **2** yielded *N*-((9*H*-fluoren-9-yl)dimethylsilyl)-6-(2-(diethylboryl)phenyl)-pyridin-2-amine (**3**). For single-crystal X-ray analysis, see Fig. S1, ESI.† Treatment of **3** with two equivalents of *n*-BuLi in toluene, followed by recrystallization from tetrahydrofuran–pentane[26] allowed isolating the ionic lithium complex (**4**) in 80% yield. For single-crystal X-ray analysis, see Fig. S2, ESI.† Direct transmetalation of **4** with $ZrCl_4$·2THF or $HfCl_4$·2THF provided the corresponding dichloro complexes **Zr-1** and **Hf-1**. Crystals suitable for X-ray crystallography were obtained from CH_2Cl_2–pentane for **Zr-1** and toluene–pentane for **Hf-1**. **Zr-1** and **Hf-1** crystalize both in the triclinic space group $P\bar{1}$. **Zr-1**: a = 884.24(6), b = 1246.31(9), c = 1610.75(12) pm, α = 105.517°, β = 91.645°, γ = 106.554°, Z = 2; **Hf-1**: a = 881.19(5), b = 1246.37(7), c = 1612.23(9) pm, α = 105.491°, β = 91.532°, γ = 106.268°, Z = 2. Both single crystal X-ray studies on **Zr-1** and **Hf-1** (Fig. 1 and 2) show that one THF is bound to the metal center leading to a trigonal bipyramidal (TB) structure with the amino-nitrogen and oxygen in the apical positions. Disordered traces of THF and CH_2Cl_2 in **Zr-1** or THF in **Hf-1** stem from solvents involved in the corresponding synthesis or recrystallization process.

An η^1-bonding of the fluorenyl moiety is observed for both **Zr-1** and **Hf-1**. This η^1-bonding fashion of the fluorenyl ligand is very unusual in group 4 complexes where usually an η^5-binding mode of a fluorenyl ligand is observed.[17,27–29] The M–N(amino) and M–C(fluorenyl) distances are 207.9/227.0 pm for **Zr-1** and 207.1/224.6 pm for **Hf-1** and are thus similar to the distances found in comparable complexes, *e.g.* in $Me_2Si(\eta^1\text{-}C_{29}H_{36})(\eta^1\text{-N-}^t\text{Bu})MCl_2(Et_2O)_2$ (M = Zr, Hf).[30] The B–N bond

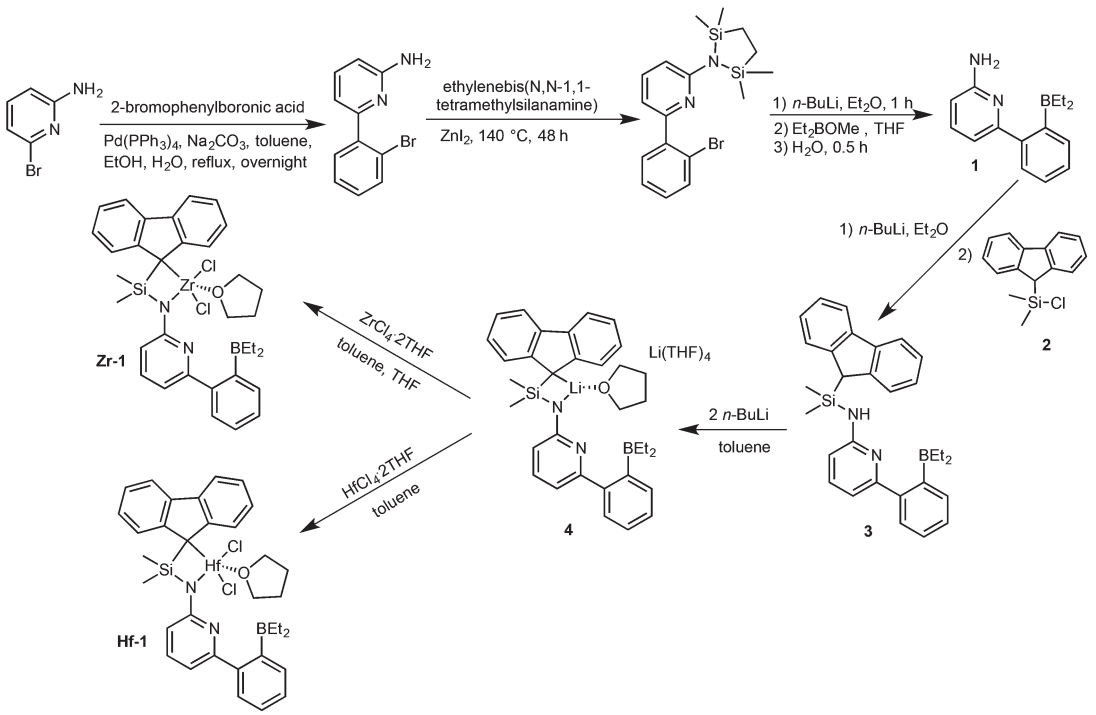

Scheme 1 Synthesis of pre-catalysts **Zr-1** and **Hf-1**.

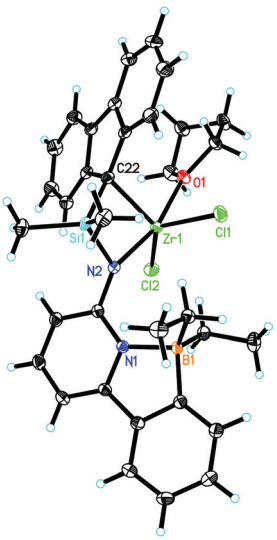

Fig. 1 Single-crystal X-ray structure of **Zr-1**. Selected bond lengths [pm] and angles [°]: Zr(1)–N(2) 207.95(10), Zr(1)–O(1) 225.02(9), Zr(1)–C(22) 227.04(12), Zr(1)–Cl(1) 237.79(4), Zr(1)–Cl(2) 241.51(3), N(1)–B(1) 165.20(17); N(2)–Zr(1)–O(1) 164.84(4), N(2)–Zr(1)–C(22) 76.12(4), O(1)–Zr(1)–C(22) 92.57(4), N(2)–Zr(1)–Cl(1) 104.63(3), O(1)–Zr(1)–Cl(1) 86.91(3), C(22)–Zr(1)–Cl(1) 99.18(3), N(2)–Zr(1)–Cl(2) 95.21, O(1)–Zr(1)–Cl(2) 84.64(3), C(22)–Zr(1)–Cl(2) 131.36(3), Cl(1)–Zr(1)–Cl(2) 128.976(13).

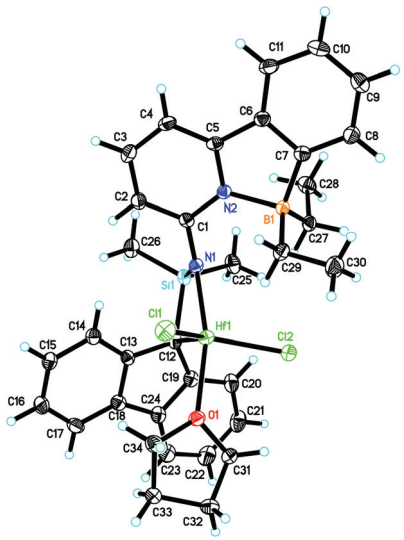

Fig. 2 Single-crystal X-ray structure of **Hf-1**. Selected bond lengths [pm] and angles [°]: Hf(1)–N(1) 207.1(2), Hf(1)–O(1) 222.29(18), Hf(1)–C(12) 224.6(2), Hf(1)–Cl(2) 234.41(7), Hf(1)–Cl(1) 239.39(7), Hf(1)–C(13) 276.7(2), Hf(1)–Si(1) 289.54(7), B(1)–N(2) 164.6(3); N(1)–Hf(1)–O(1) 164.14(8), N(1)–Hf(1)–C(12) 76.43(9), O(1)–Hf(1)–C(12) 91.65(8), N(1)–Hf(1)–Cl(2) 104.79(6), O(1)–Hf(1)–Cl(2) 87.66(5), C(12)–Hf(1)–Cl(2) 101.61(7), N(1)–Hf(1)–Cl(1) 95.24(6), O(1)–Hf(1)–Cl(1) 84.49(5), C(12)–Hf(1)–Cl(1) 130.49(7), Cl(2)–Hf(1)–Cl(1) 127.39(3).

length is 165.2 pm for **Zr-1**, which is slightly longer than the one in dimethylsilylene-bis(6-[2-(diethylboryl)phenyl]pyrid-2-ylamido)$ZrCl_2$ (**Zr-4**, 163.5 pm).[3] An explanation for this slight

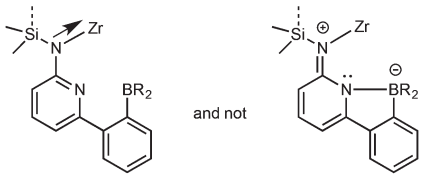

Fig. 3 Preferred resonance structure in **Zr-1**.

lengthening of the N–B bond is an increased electrophilic character of the metal in **Zr-1** caused by the weaker electron-donation ability of the η^1-bound fluorenyl ligand. This results in a reduced electron density at the pyridine, which directly translates into a decreased coordination ability of the pyridine nitrogen to the boron and consequently a longer intramolecular N–B bond (Fig. 3).

Synthesis of pre-catalyst Zr-2

As described in Scheme 2, 6-[2-(dimesitylboryl)phenyl]pyridin-2-amine (**5**)[31,32] was prepared in analogy to compound **1** in 42% isolated yield.

Deprotonation of **5** in THF produced the lithium complex **6** with two THF molecules coordinated to lithium. Subsequent reaction with chlorodimethyl(2,3,4,5-tetramethylcyclopenta-2,4-dienyl)silane and recrystallization from diethyl ether–pentane allowed isolating compound **7** in 94% yield. Double deprotonation of **7** and combination with $ZrCl_4$·2THF provided **Zr-2** in 32% isolated yield. Crystals suitable for single-crystal X-ray diffraction were obtained from toluene–pentane. **Zr-2** (Fig. 4) crystalizes in the triclinic space group $P\bar{1}$ with a = 993.61(7), b = 1247.23(8), c = 1590.00(11) pm, α = 84.293°, β = 73.108°, γ = 83.935°, Z = 2.

The cyclopentadienyl ligand is η^5-bound to Zr(1); the Zr(1)–N_{amide} distance is 210.85(10) pm and thus longer than in **Zr-1** (207.9 pm). In stark contrast to **Zr-1**, the nitrogen in the pyridyl ring is coordinated to zirconium (Zr(1)–N(2) 249.61(9) pm) and no coordination to the boron atom exists, at least in the solid state. For the structure in solution, *vide infra.* The absence of any N–B bonding in **Zr-2** is attributed to the pronounced steric demand of the two mesityl groups at boron compared to the two small ethyl groups in **Zr-1**. The absence of any coordinated solvent to the metal is attributable to a weakly but still significantly intramolecular stabilization of the electrophilic metal center by the pyridine ring through the N(2)–Zr(1) bond, which becomes also evident from its single crystal X-ray structure.

Synthesis of pre-catalyst Zr-3

The borylamine-free model catalyst **Zr-3** was prepared as is shown in Scheme 3. 6-(2-(2-Propyl)phenyl)pyrid-2-ylamine was prepared *via* Pd-mediated coupling of 2-amino-6-bromopyridine with 2-isopropylphenylboronic acid, Deprotonation with *n*-BuLi followed by reaction with compound **2** yielded ligand **8**. Double deprotonation of **8** yielded the lithium complex **9**, which could not be isolated as a stable compound. However,

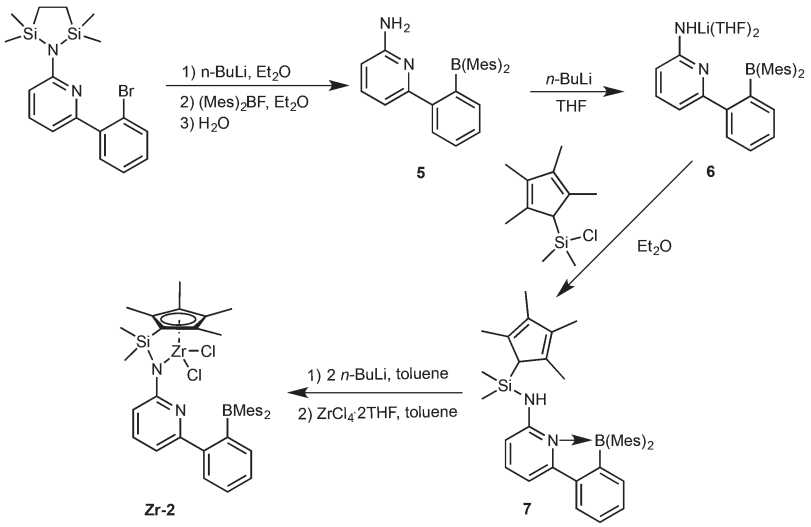

Scheme 2 Synthesis of pre-catalyst **Zr-2**.

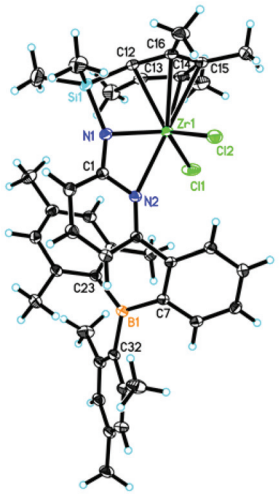

Fig. 4 Single-crystal X-ray structure of **Zr-2**. Selected bond lengths [pm] and angles [°]: Zr(1)–N(1) 210.85(10), Zr(1)–Cl(1) 239.60(3), Zr(1)–Cl(2) 242.19(4), Zr(1)–C(13) 245.26(11), Zr(1)–C(12) 245.60(11), Zr(1)–N(2) 249.61(9), Zr(1)–C(16) 254.07(11), Zr(1)–C(14) 256.92(12), Zr(1)–C(15) 258.66(12); N(1)–Zr(1)–Cl(1) 124.37(3), N(1)–Zr(1)–Cl(2) 108.44(3), Cl(1)–Zr(1)–Cl(2) 109.597(13), N(1)–Zr(1)–N(2) 57.42(3), Cl(1)–Zr(1)–N(2) 86.51(2), Cl(2)–Zr(1)–N(2) 86.10(2).

in situ formation and reaction with $ZrCl_4$·2THF allowed isolating analytically pure **Zr-3**.

Variable-temperature ^{11}B NMR measurements

^{11}B NMR measurements[33–35] at different temperatures on **Zr-1** and **Zr-2** were carried out in a temperature range of 0–80 °C. **Zr-1** shows a sharp peak at $\delta \sim 6$ ppm (Fig. S3†), which is typical for tetracoordinated borane in accordance with its single-crystal X-ray structure.

Once the temperature is increased from 0 to 80 °C, the signal shifts from δ = 6.3 to 4.7 pm. The pyridine nitrogen remains bound to the boron forming a Lewis acid/base pair that does not dissociate up to 80 °C, which is indicative of a strong binding and a high-energy barrier to break the N–B bond. After the addition of MAO, the ^{11}B NMR shows the signal of tetracoordinated borane ($\delta \sim -5$ ppm) and, above 30 °C, a new (weak) boron peak at $\delta \sim 87$ ppm (Fig. S4†), which can be assigned to tricoordinated borane. Clearly, in the presence of MAO the N–B bond starts to dissociate above 30 °C, though to a low degree. Upon addition of NBE to a toluene-d_8 solution of **Zr-1**/MAO, a very weak peak at $\delta \sim$ 85 ppm, which can be assigned to tricoordinated borane, becomes visible (Fig. S5†). Evidently, the system contains predominantly tetracoordinated borane moieties. For implications on reactivity, *vide infra*.

In ligand **7**, the N–B bond exists in solution as evidenced by the chemical shift for boron at $\delta = -0.52$ ppm in the ^{11}B NMR (Fig. S6†), which is assignable to a tetracoordinated borane (*vide infra*).[33–35] In contrast to the solid-state structure, in solution above 10 °C both free and nitrogen-coordinated borane are observed for **Zr-2** in toluene-d_8 as indicated by two peaks around $\delta \sim 76$ (tricoordinated borane) and ~5 ppm (tetracoordinated borane) in the ^{11}B NMR spectrum (Fig. S7†). These findings clearly show that in solution there exists an equilibrium between a closed and open structure for **Zr-2**. The ^{11}B NMR of **Zr-2**/MAO and **Zr-2**/MAO/NBE (Fig. S8 and S9†) display two boron peaks similar to those of **Zr-2** except that the tetracoordinated species become more abundant.

The ^{11}B NMR of **Hf-1** shows the signals for tetracoordinated borane at δ = 6 and 4 ppm above 25 °C (Fig. S10†); the absence of any tricoordinated borane again indicates a strong N–B bond. The ^{11}B NMR of **Hf-1**/MAO is characterized by one signal for tricoordinated borane at δ = 87 ppm and two signals for tetracoordinated borane at δ = 4 and −2 ppm (Fig. S11†). For

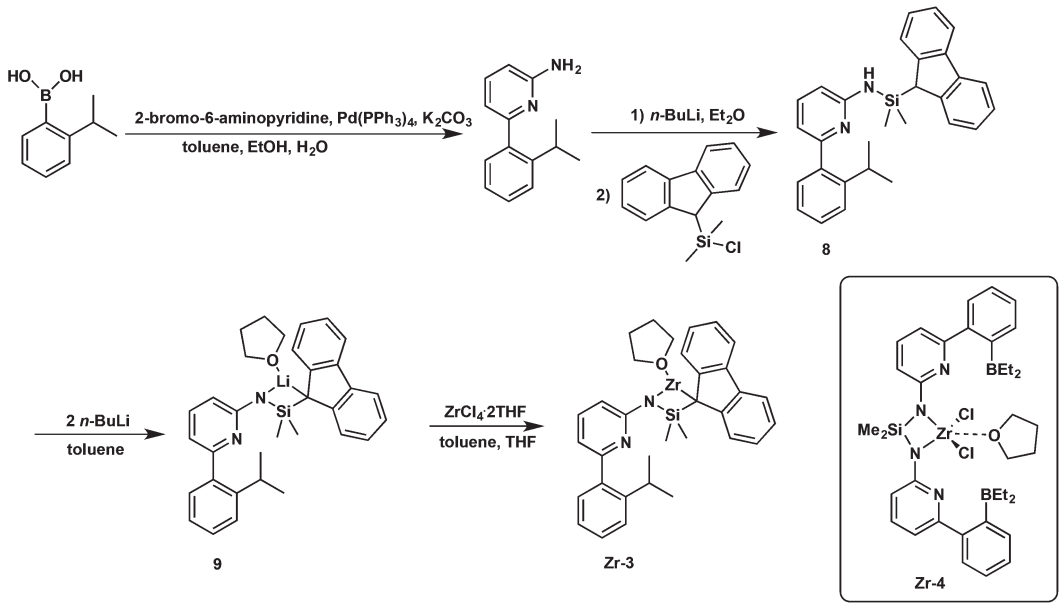

Scheme 3 Synthesis of pre-catalyst **Zr-3**.

Hf-1/MAO/NBE two sets of signals at $\delta \sim 4$ and 1 ppm, both typical for tetracoordinated borane and at $\delta \sim 87$ ppm for tricoordinated borane is observed (Fig. S12†). The peak at $\delta \sim 1$ ppm is invisible while a new peak at $\delta \sim 85$ ppm is observed at $T \geq 60$ °C.

Norborn-2-ene (NBE) homopolymerization and copolymerization of ethylene (E) with NBE

Catalysts **Zr-1**, **Zr-2**, **Zr-3** and **Hf-1** were activated with MAO and used in the homopolymerization of NBE. While the model catalyst **Zr-3** did not produce any appreciable amount of poly-NBE, **Zr-1**, **Zr-2** and **Hf-1** allowed for the synthesis of the target polymer (Table 1).

Both **Zr-1** and **Zr-2** produced high molecular weight poly(NBE), albeit with low productivity. Interestingly, polymers with an extraordinary high *cis*-content (up to 95%) were obtained (Fig. S13–S16, ESI†). The measured T_g values are in line with those for high *cis* poly(NBE). Importantly, poly(NBE) prepared by the action of **Hf-1** contains both ROMP and, to a very minor extent, VIP-derived sequences (Fig. S17 and S18 ESI†). Also, productivities are substantially higher than those for **Zr-1** and **Zr-2**. Also in line with a VIP-derived polymer block, the T_g values are higher than those of **Zr-1** and **Zr-2**-derived poly(NBE). The data presented here clearly show that catalysts **Zr-1**, **Zr-2**, **Hf-1** containing the 6-[2-(R_2B)phenyl]pyrid-2-ylamido motif are ROMP active, while systems that lack this motif are not (**Zr-3**).

Next, to check for their VIP/ROMP propensity, catalysts **Zr-1**, **Zr-2**, **Zr-3** and **Hf-1**, all activated by MAO, were used in the copolymerization of E with NBE. Polymerization results are summarized in Table 2.

With **Zr-1**/MAO (Table 2, entries 1–7), activity decreased with increasing NBE concentration. This effect can be counterbalanced by an increase in E-pressure. Up to 29.3 mol% of NBE could be incorporated into the copolymer. The ^{13}C NMR spectrum (Fig. 5) shows the characteristic signals for both alternating (E-NBE-E-NBE) and isolated sequences (E-NBE-E-E) at δ = 47.8, 47.2 (C_2/C_3), 42.0, 41.5 (C_1/C_4), 33.0 (C_7) and

Table 1 Results for NBE homopolymerization by **Zr-1**, **Zr-2** and **Hf-1** activated by MAO[a]

#	Cat.	T (°C)	Productivity[b]	M_n [c] (g mol^{-1})	PDI[c]	T_g [d] (°C)	*cis*[e] (%)	Type
1	**Zr-1**	50	5	40 000	1.2	35	75	ROMP
2	**Zr-1**	65	6	160 000	1.4	48	90	ROMP
3	**Hf-1**	50	42	120 000	2.1	55	96	VIP : ROMP = 0.3 : 100
4	**Hf-1**	65	18	52 000	2.6	55	90	VIP : ROMP = 0.9 : 100
5	**Zr-2**	50	5	120 000	2.5	45	86	ROMP
6	**Zr-2**	65	7	200 000	1.5	37	95	ROMP

[a] 100 mL Schlenk flask, total volume of reaction mixture: 50 mL of toluene, [catalyst] = 1×10^{-4} mol L^{-1}, catalyst : MAO : NBE = 1 : 2000 : 10 000, t = 1 h. [b] Activity in kg of polymer mol$^{-1}_{\text{catalyst}}$ h^{-1}. [c] HT-GPC in 1,2,4-trichlorobenzene *vs.* PS. [d] Measured by DSC. [e] Determined by ^{13}C NMR analysis in 1,1,2,2-tetrachloroethane-d_2.

Table 2 E-NBE copolymerization results for **Zr-1**, **Hf-1**, **Zr-2** and **Zr-3** activated by MAO[a]

#	Cat.	M : MAO : NBE	T/p (°C)/bar	A^b	$C_{ROMP}{}^c$ (mol-%)	$C_{VIP}{}^c$ (mol%)	$M_n{}^d$ (g mol^{-1})	PDI^d	$T_m{}^e$ (°C)
1	**Zr-1**	1 : 2000 : 10 000	50/2	55	0	14.2	290 000	1.9	123
2	**Zr-1**	1 : 2000 : 10 000	50/4	45	0	29.3	>6 000 000	—	128
3	**Zr-1**	1 : 2000 : 20 000	50/2	10	0	6.6	330 000	4.1	123
4	**Zr-1**	1 : 2000 : 20 000	50/4	9	0	6.8	>6 000 000	—	124
5	**Zr-1**	1 : 2000 : 20 000	50/6	27	0	10.7	360 000	3.2	124
6	**Zr-1**	1 : 2000 : 20 000	65/4	24	0	4.3	210 000	3.6	123
7	**Zr-1**	1 : 2000 : 20 000	80/4	19	0	7.3	150 000	4.8	127
8	**Hf-1**	1 : 2000 : 10 000	50/4	7	0	6.5	>6 000 000	—	126
9	**Hf-1**	1 : 2000 : 20 000	50/4	6	0	18.1	430 000	3.7	126
10	**Zr-3**	1 : 2000 : 10 000	50/4	73	0	4.1	>6 000 000	—	129
11	**Zr-3**	1 : 2000 : 20 000	50/4	68	0	3.0	>6 000 000	—	129
12	**Zr-2**	1 : 2000 : 10 000	50/4	1	6	3	>6 000 000	—	130
13	**Zr-2**	1 : 2000 : 20 000	30/4	2	11	8	>6 000 000	—	131
14	**Zr-2**	1 : 2000 : 20 000	50/4	1	21	7	>6 000 000	—	129
15	**Zr-2**	1 : 2000 : 20 000	65/4	6	0	2.7	>6 000 000	—	132
16	**Zr-2**	1 : 2000 : 20 000	80/4	4	0	2.5	>6 000 000	—	129

[a] 250 mL of toluene (including the volume of monomer), t = 1 h, [catalyst] = 2 × 10^{-5} mol L^{-1}. [b] Activity in kg of polymer mol$^{-1}{}_{catalyst}$ h^{-1} bar^{-1}. [c] NBE content (ROMP and VIP) in the copolymer [mol%] as estimated by ^{13}C NMR spectroscopy. [d] HT-GPC in 1,2,4-trichlorobenzene *vs.* PS. [e] Measured by DSC.

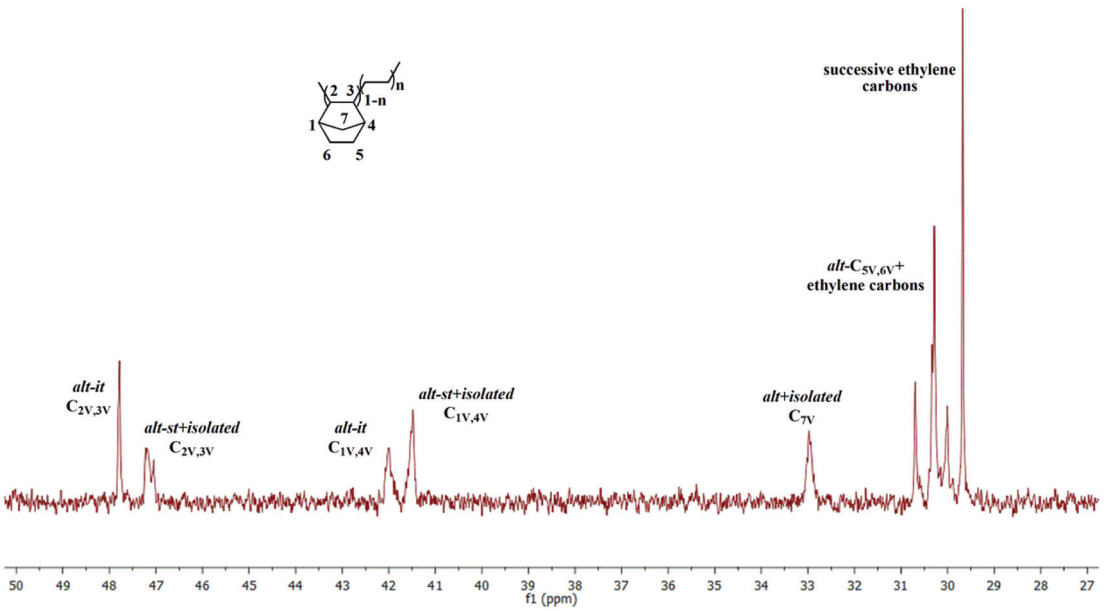

Fig. 5 ^{13}C NMR spectrum of poly(E)-*co*-poly(NBE)$_{VIP}$ produced by **Zr-1**/MAO (Table 2, entry 2) (in 1,1,2,2-tetrachloroethane-d$_2$).

30.7–29.7 ppm (C_5/C_6, PE).[36,37] While one cannot distinguish between alternating syndiotactic (*alt-st*) and isolated NBE sequences and therefore not judge on the extent of syndiotacticity, the alternating isotactic (*alt-it*) units are those that must be expected from a centrosymmetric catalyst such as **Zr-1**. Signals for NBE diads (E-NBE-NBE-E) or even NBE triads (E-NBE-NBE-NBE-E) were absent. None of these copolymers showed signals for ROMP-derived poly(NBE). For the copolymers obtained by the catalytic system **Hf-1**/MAO, up to 18.1 mol% VIP-derived poly(NBE) was realized at high NBE concentration (Table 2, entry 9, Fig. S19†). Generally, catalytic activities were lower than those for **Zr-1**/MAO. Again, no signals for ROMP-derived poly(NBE) were found in these copolymers. As anticipated, the aminoborane motif-free catalyst **Zr-3** also produced only VIP-derived poly(NBE)-*co*-poly(E), albeit with a lower NBE incorporation (Table 2, entries 10 and 11, Fig. S20†) compared to **Zr-1** under identical conditions (Table 2, entries 2 and 4). However, activities were higher than those by **Zr-1**/MAO, probably due to the sterically less encumbered nature of **Zr-3**.

In contrast to **Zr-1** and **Hf-1**, **Zr-2** allows the synthesis of copolymers containing blocks of both ROMP- and VIP-derived poly(NBE) sequences in the same polymer chain. At low NBE concentration ([NBE] = 0.2 mol L^{-1}), poly(NBE)$_{ROMP}$-*co*-poly-

$(NBE)_{VIP}$-*co*-poly(E) with a block ratio of 6 : 3 : 91 (Table 2, entry 12, Fig. S21†) was obtained. An increase in NBE concentration ([NBE] = 0.4 mol L^{-1}) resulted in a further increase in the proportion of ROMP- and VIP-derived poly(NBE) units with ratios of 11 : 8 : 81 and 21 : 7 : 72 (Table 2, entries 13 and 14, Fig. S22 and S23†) at 30 and 50 °C, respectively. An increase in polymerization temperature to 65 °C and 80 °C produced VIP-derived poly(NBE)-*co*-poly(E) with 2.7 mol% and 2.5 mol% NBE incorporation (Fig. S24†). Notably, the molecular weights of these copolymers were all >6 000 000 g mol^{-1}. Such high molecular weights are indicative for polymerizations with almost no β-hydride elimination or transfer to monomer.

In order to shed light on the polymer structure, the ^{13}C NMR spectrum of poly$(NBE)_{ROMP}$-*co*-poly$(NBE)_{VIP}$-*co*-poly(E) was compared to the one of poly$(NBE)_{ROMP}$ and poly$(NBE)_{VIP}$-*co*-poly(E) (Fig. 6). Signals at δ = 47.0 ($C_{2,3}$), 41.5 ($C_{1,4}$), 32.9 (C_7) ppm are assignable to *alt-st*/isolated VIP-derived E-NBE sequences while the one at δ = 29.7 ppm corresponded to PE sequences. Signals at δ = 47.8 and 41.9 ppm, which could be assigned to *alt-it* E-NBE diads, were absent. Most importantly, signals at δ = 134.2, 42.8, 38.8 and 33.5 ppm that can unambiguously be assigned to poly$(NBE)_{ROMP}$ were observed even after the extraction by THF, which is known to dissolve pure ROMP-derived poly(NBE).

All together, poly$(NBE)_{ROMP}$-*co*-poly$(NBE)_{VIP}$ sequences must be present in the same polymer chain, which suggests the incorporation of ROMP-derived poly(NBE) units in the chain through an α-H elimination process. Further evidence comes from the absence of any glass transition attributable to a poly$(NBE)_{ROMP}$ homopolymer. Most vinylic carbons in the segment of the ROMP-type poly(NBE), surprisingly, were observed in the *cis*-configuration, signals at δ = 133.1 or 43.2 ppm belonging to *trans*-$C_{2,3}$ or $C_{1,4}$ repeat units were almost invisible. For mechanistic implications, *vide infra*.

In contrast to poly$(NBE)_{ROMP}$-*co*-poly$(NBE)_{VIP}$-*co*-poly(E) prepared by the action of (η^5-tetramethylcyclopentadienyl)dimethylsilyl(6-[2-(*diethyl*boryl)phenyl]pyrid-2-yl)amido-$TiCl_2$,[2] **Zr-2** containing the more bulky 6-[2-(dimesitylboryl)phenyl]-pyrid-2-ylamido motif allows only for lower NBE incorporation, which further supports the argument about sterics. Also in line with increased sterics, higher molecular weights (M_n > 6 000 000 g mol^{-1}) were obtained with **Zr-2**/MAO.

Discussion

As outlined above, both tri- and tetracoordinated boranes are present in **Hf-1**/MAO and **Hf-1**/MAO/NBE (Fig. S11 and S12†). Once MAO is added to **Hf-1**, the formation of methane occurs in the temperature range of 25–80 °C (Fig. S25†). At 60 °C, ethylene becomes visible, too. Notably, at 25 °C, a weak but detectable signal for a Hf-alkylidene at δ = 8.60 ppm (d, J = 8 Hz) can be observed. A terminal vinyl group can be identified at δ = 4.92 and 5.73 ppm in the range of 25–80 °C (Fig. 7 and

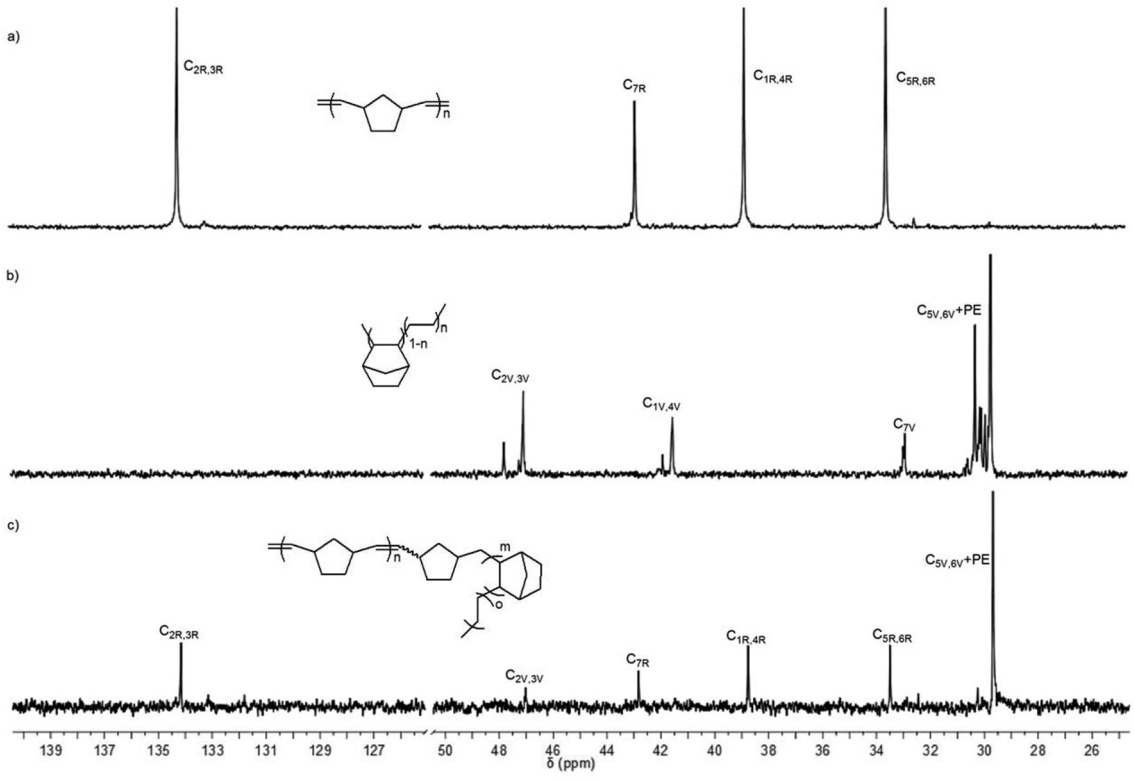

Fig. 6 ^{13}C NMR spectra of (a) poly$(NBE)_{ROMP}$, (b) poly$(NBE)_{VIP}$-*co*-poly(E) (Table 1, entry 1) and (c) poly$(NBE)_{ROMP}$-*co*-poly$(NBE)_{VIP}$-*co*-poly(E) (Table 1, entry 14) in 1,1,2,2-tetrachloroethane-d_2.

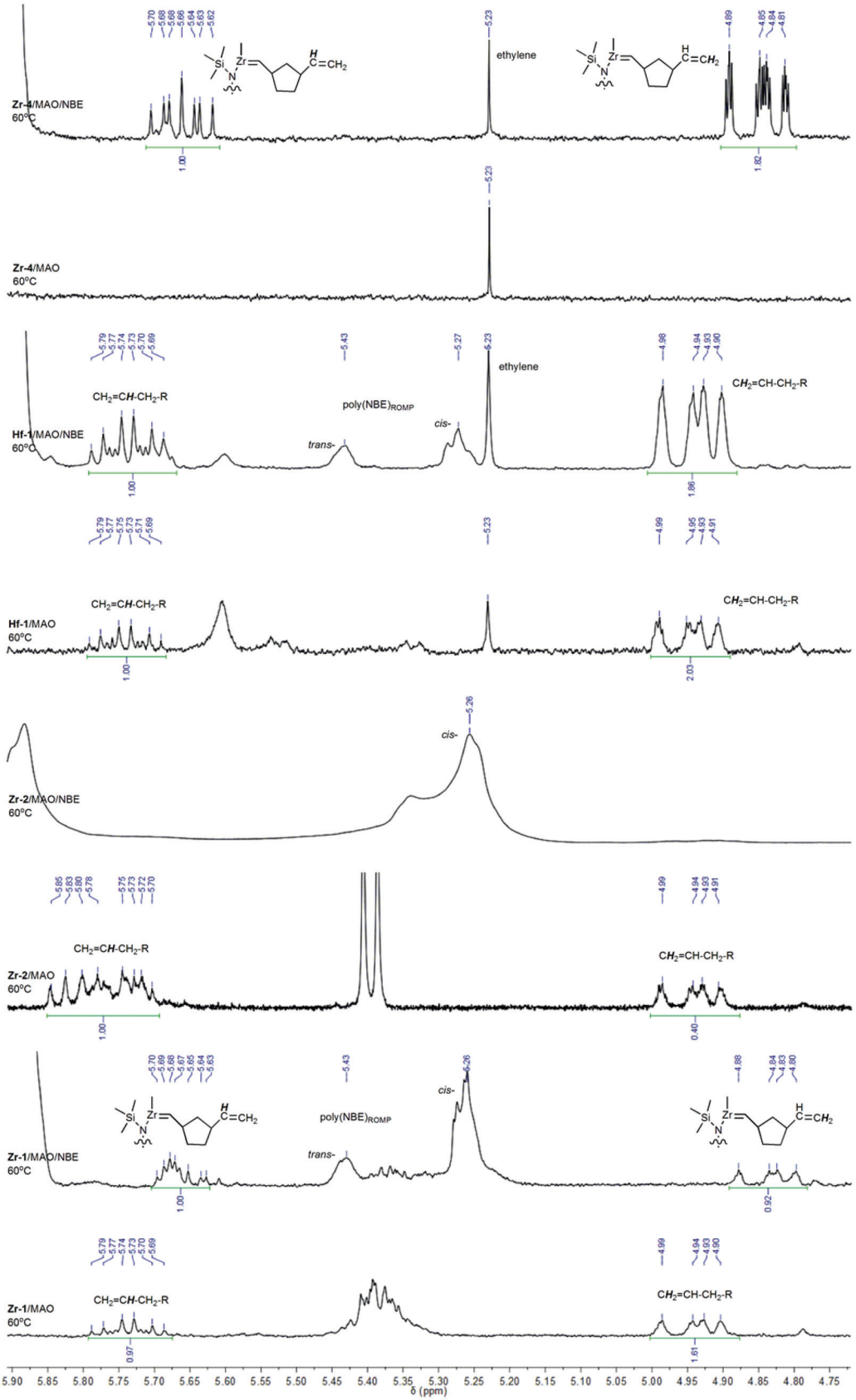

Fig. 7 ^{1}H NMR spectra of catalyst/MAO and catalyst/MAO/NBE in toluene-d_8 at 60 °C (4.7–5.9 ppm).

S26b†). The signal at δ = 5.73 ppm can clearly be assigned to a CH_2═C*H*–CH_2–R species (for a comparison with 1-octene see Fig. S26a†). The ^{1}H NMR spectrum of **Hf-1**/MAO/NBE shows weak but detectable signals assignable to a Hf-methylidene at 25 °C at δ = 8.58 (d, J = 8 Hz) and 8.49 ppm (d, J = 8 Hz, Fig. S27†). Ethylene (δ = 5.24 ppm at 40 °C) can only be observed at T > 25 °C. Methane (δ = 0.16 ppm at 25 °C) is produced in the range of 25–80 °C. The above-mentioned terminal vinyl group at δ = 4.92 and 5.73 ppm (CH_2═CH–CH_2–R species) remains visible in the range of 25–80 °C (Fig. S28†).

It changes only slightly in intensity while ROMP-derived poly(NBE) (δ = 5.26 (*cis*) and 5.43 ppm (*trans*)) formed slowly but steadily. Thus, upon activation with MAO, **Hf-1** must form a VIP-active, cationic species that quickly consumes the E that is present in the system. α-Hydrogen elimination results in the formation of a Hf-alkylidene, which upon reaction with E forms a Hf-methylidene and vinyl-terminated oligoethylenes. These two reaction products are visible in the spectrum. The Hf-methylidene then starts the ROMP of NBE. The low ROMP propensity of **Hf-1** explains why only VIP-derived poly(NBE)-*co*-poly(E) is produced in the copolymerization of E with NBE.

As outlined above, the boron in **Zr-1** is fully coordinated to the nitrogen both in the solid state and in solution. Upon addition of MAO or MAO/NBE, the borane remains mostly tetracoordinated, however, some tricoordinated species become visible, too (Fig. S4 and S5†). This rather small amount of tricoordinated borane translates into a small amount of free pyridine, which in the presence of MAO is capable of starting the ROMP of NBE at elevated temperatures (Fig. S13 and S14†). However, in case ethylene is present at the same time, no ROMP-derived structures are observed. Obviously, similar to **Hf-1**, most of the catalyst forms a cationic alkyl complex after activation with MAO, resulting in poly(NBE)$_{VIP}$-*co*-poly(E). Upon treatment of **Zr-1** with MAO at −60 °C, methane (δ = 0.26 ppm at −60 °C, 0.17 ppm at 20 °C) starts to evolve, a process that becomes more visible with increasing temperature. Clearly, the corresponding cationic RR′Zr^+–CH_2–Al(CH_3)–O– species forms from RR′Zr^+–CH_3 and MAO (Fig. S29 and S30†). **Zr-1**/MAO at 60 °C also shows vinyl-terminated oligoethylenes (Fig. 7). In the presence of NBE, small amounts of poly(NBE)$_{ROMP}$ starts to form at −10 °C (*cis* : *trans* = 80 : 20) again accompanied by the formation of methane (Fig. S31 and S32†). No Zr-alkylidene is observed, probably because its concentration is too low. **Zr-1**/MAO/NBE at 60 °C again shows terminal vinyl groups, however, with somewhat different chemical shift and multiplicity for the signal at δ = 5.67 ppm (Fig. 7). In addition, numerous signals for poly(NBE)$_{ROMP}$ become visible (Fig. 7). This terminal vinyl group is believed to result from the reaction of a Zr-methylidene with NBE. For a detailed discussion of this reaction sequence with **Zr-4**, *vide infra*.

In contrast to **Zr-1**, the pyridyl group in **Zr-2** is *not* coordinated to the boron in the solid state. In solution, equally substantial and comparable amounts of tri- and tetracoordinated boranes are observed, both in the absence and presence of MAO and NBE (Fig. S7–S9†). Upon activation with MAO an active cationic species forms *via* release of methane (Fig. S33 and S34†). Larger fractions of free pyridine favor α-H-elimination and in the presence of NBE and predominantly *cis*-poly(NBE)$_{ROMP}$ forms even at −50 °C (Fig. S35†). This is why **Zr-2**/MAO in the presence of both E and NBE produces poly(NBE)$_{VIP}$-*co*-poly(NBE)$_{ROMP}$-*co*-poly(E). No methane is visible even at elevated temperature. Again, no Zr-alkylidene is observed. With **Zr-4**, which contains two 6-[2-(diethylboryl)-phenyl]pyrid-2-yl groups (Scheme 3), the reaction sequence from a VIP- to a ROMP-active species can be followed best. There, homopolymerization of NBE at 60 °C by MAO-activated **Zr-4** applying a ratio of **Zr-4**/MAO/NBE = 1 : 2000 : 20 000 results in poly(NBE)$_{ROMP}$ (M_n = 93 000 g mol^{-1}, PDI = 1.6, *cis* : *trans* = 10 : 90, Fig. S36†). Copolymerization of E with NBE at 60 °C using **Zr-4**/MAO/NBE in a ratio of 1 : 2000 : 20 000, $p_{ethylene}$ = 4 bar reportedly yielded poly(NBE)$_{ROMP}$-*co*-poly(NBE)$_{VIP}$-*co*-poly(E) = 3 : 13 : 84 (M_n = 230 000 g mol^{-1}, PDI = 1.6).[3] **Zr-4**/MAO at 60 °C shows no terminal vinyls but ethylene (Fig. 7). In the presence of NBE, a terminal vinyl group adjacent to a 1,3-cyclopentylen ring, –(*c*-1,3-C_5H_8)–CH═CH_2, is observed (Fig. 7). The signal for the terminal CH-group at δ = 5.67 ppm (ddd, J = 7.1 Hz, J = 10.1 Hz, J = 17.4 Hz) unambiguously proofs this structural motif. Since the signals for poly(NBE)$_{ROMP}$ are completely absent, this structural motif cannot result from a cross metathesis of a ROMP-active, propagating Zr-alkylidene but must stem from the reaction of a Zr-methylidene with NBE.

Following the reaction of **Zr-4** with MAO and NBE by NMR suggests that upon addition of MAO to **Zr-4** in toluene-d_8 in a molar ratio of **Zr-4**:MAO = 1 : 30 at −60 °C, the cationic species II (Scheme 4) forms. Potentially, it can be stabilized by the coordination of the pyridine nitrogen. II can further react with MAO to produce III (Scheme 4) and methane (δ = 0.17 ppm at 20 °C, Fig. S37 and S38†).[38–41] At −20 °C, the dormant species III, which is inactive in polymerization, becomes visible in the ^{1}H NMR (δ_{CH2} = 0.82 ppm at 20 °C). A further increase in temperature to 20 °C results in α-H elimination and a ROMP-active Zr-alkylidene (V, Scheme 4) forms from II as evidenced by the alkylidene signal visible at δ = 8.6 ppm in the ^{1}H NMR (Fig. S37†).[3,42–44] In line with that, at 30 °C, ^{11}B NMR shows apart from the parent tetracoordinated B atom (δ = 2.6 ppm) the formation of a tricoordinated species at δ = 86.7 ppm (Fig. S39 and S40†) indicating the dissociation of the N–B bond. This strongly suggests that the opening of the N–B bond generates a sufficient fraction of free pyridine moiety that induces α-H elimination. Substantial fractions of this ROMP-active Zr-alkylidene (V) experience bimolecular decomposition, resulting in the formation of ethylene at $T \geq$ 30 °C (Scheme 4). Thus, the signal for ethylene is clearly observed at δ = 5.25 ppm in the ^{1}H NMR at $T \geq$ 30 °C (Fig. S37†). For **Zr-4**/MAO/NBE (**Zr-4** : MAO : NBE = 1 : 30 : 10), a zirconium alkylidene (Zr = CHR)[42,44–46] is observed in the ^{1}H NMR at δ = 8.5 ppm at 20 °C (Fig. S41 and S42†). In case **Zr-4** (or **Zr-2**) starts first vinyl insertion copolymerization of E with NBE, insertion of NBE followed by α–H elimination promoted by the pyridine nitrogen through a six-membered transition state produces the Zr-alkylidene VI-P from V-P (Scheme 4), which is the

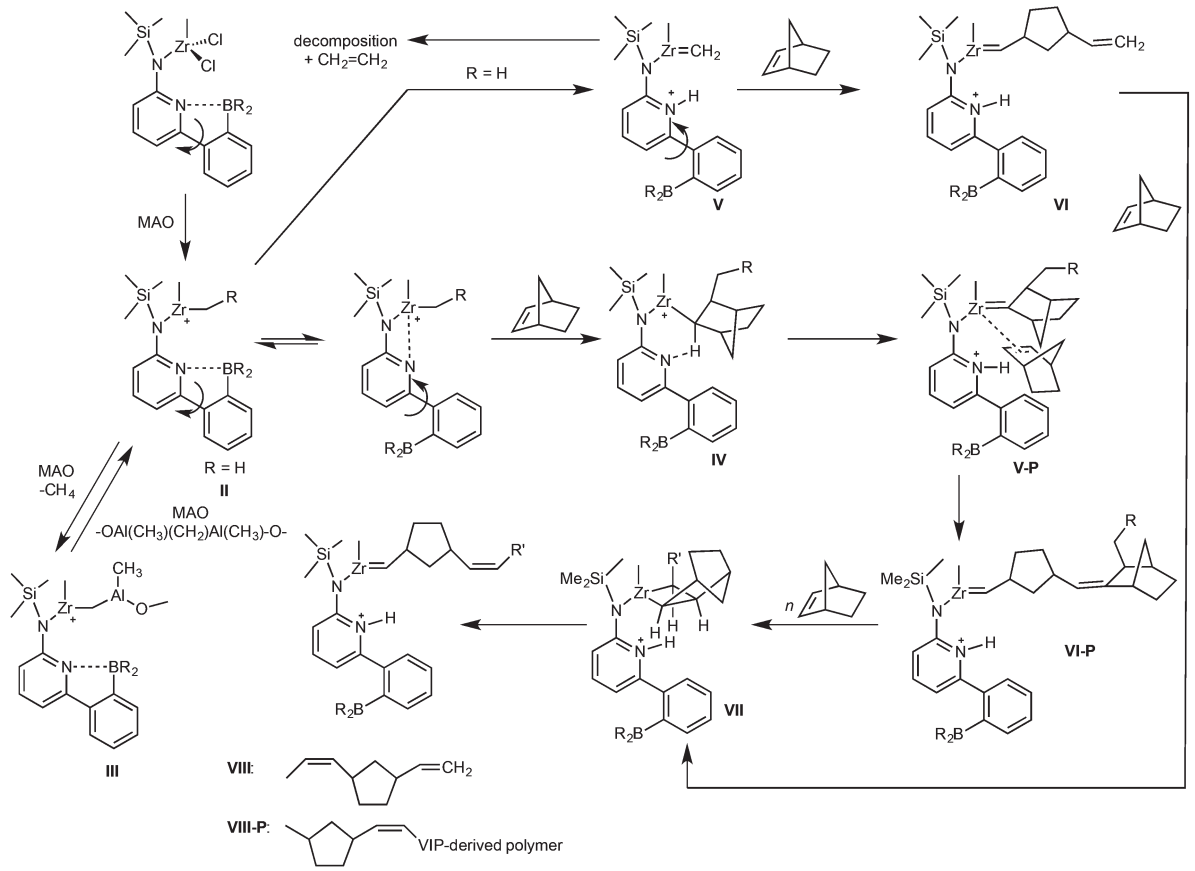

Scheme 4 Proposed mechanism for the switch from VIP to ROMP. P = polymer.

ROMP-active species. Competition between the insertion of NBE and the re-formation of the N–B bond is proposed. As observed for **Zr-1**/MAO/NBE, a terminal vinyl end group (VI, Scheme 4) formed *via* reaction of $Zr{=}CH_2$ with NBE can be clearly seen in the ^1H NMR at δ = 4.86 and 5.67 ppm (Fig. S43†). Concomitantly, apart from tetracoordinated borane at δ = 2.8 ppm, tricoordinated borane can be observed by ^{11}B NMR at δ = 86.8 ppm at $T \geq 30$ °C (Fig. S44†). Notably, at $T \geq 60$ °C, a second tricoordinated B species appears in the ^{11}B NMR at δ = 84.3 ppm and grows in intensity with increasing temperature. So far, this tricoordinated B-species cannot be assigned to a specific intermediate. High NBE concentrations were found to stabilize the metal alkylidene in both **Zr-2** and **Zr-4** and to encourage ROMP of NBE resulting in high proportion of ROMP-derived poly(NBE) units in the polymer (Table 2, entries 12 and 14). *Vice versa*, ethylene pressures > 4 bar shift the reaction from ROMP towards VIP.[1–3,15,16]

All together, the data presented here are in line with our previous proposal,[2,3,15,16] which show that only high NBE concentrations promote the ROMP process. Notably, Zr-alkylidenes cannot be isolated unless hexacoordinated species containing chelating ligands are formed.[45] As surmised earlier,[15] a crowded ligand sphere around the metal as found in **Zr-2** favors this α-H elimination process, *i.e.* the switch from VIP to ROMP. The low propensity of pyridine to coordinate to boron in **Zr-2** clearly stems from the sterics provided by the mesityl groups, which together with the η^5-tetramethylcyclopentadienyl (Cp*) ligand simply prevents any extensive coordination. This and the fact that **Zr-3** without a 6-(2-BR_2-phenyl)pyrid-2-yl group does not show any ROMP-activity, neither for NBE nor for E-NBE, strongly support an involvement of the pyridyl group and an α-H abstraction process triggered by the pyridine. In view of these sterics, it is also not surprising at all that **Hf-1** with minor steric constraints around the metal shows no tendency to switch from VIP to ROMP in the presence of E regardless of VIP- and ROMP-derived poly(NBE) obtained in NBE homopolymerization (Fig. S17 and S18†). Finally, the high *cis*-selectivity of **Zr-2** is a result of the large dimesitylboryl group, which forces NBE to add to VI-P in the outlined way to from VII (Scheme 4, Fig. S15 and S16†).

Conclusions

In the copolymerization of E with NBE, **Zr-2**, which has mesityl substituents at the boron and a crowded ligand sphere around the metal, allows the *cis*-selective synthesis of copolymers containing both ROMP- and VIP-derived poly(NBE) units within a single polymer chain resulting in a poly(NBE)$_{ROMP}$-*co*-poly(NBE)$_{VIP}$-*co*-poly(E) structure through a switch from VIP to

ROMP. In the presence of E, both **Zr-1** and **Hf-1** show no tendency to undergo α-H elimination producing solely VIP-derived poly(NBE)-*co*-poly(E) with up to 29.3 mol% NBE incorporation. We attribute the low propensity of both **Zr-1** and **Hf-1** to promote ROMP to the instability of any metal alkylidene in the presence of E. As expected and in line with previous findings, the aminoborane-free model catalyst **Zr-3** results in the formation of poly(NBE)$_{VIP}$-*co*-poly(E) copolymers, which again supports the crucial role of the 6-[2-(R_2-boryl)-phenyl]pyrid-2-ylamido ligand in the α-H abstraction process. Variable-temperature ^{1}H and ^{11}B NMR allow correlating the propensity of a pre-catalyst activated by MAO to form tricoordinated borane with its propensity to produce ROMP-derived structures inside the copolymer. A detailed study on **Zr-4** offers insight into important intermediates and confirms the proposed mechanism. Current efforts concentrate on detailed NMR studies and ^{13}C-labelled NBE to shed more light on the role of borylamino group. The studies outlined here clearly support the formation of a Zr-methylidene in the ROMP of NBE *via* pyridine-induced α-H abstraction. Besides of the 6-(2-BR2-phenyl)pyrid-2-yl motif,[1,16] the proposed crucial role of the bulky tetramethylcyclopentadienyl (Cp*) moiety in the α-H abstraction in *ansa*-type half sandwich complexes has been confirmed. Apart from sterically enforcing a switch from VIP to ROMP, the Cp* ligand as a six-electron donor can sterically and maybe also electronically stabilize[44] the metal alkylidene and thus promote the ROMP of cyclic olefins. Whether the strong Lewis base character of the Cp* moiety also favors α-proton abstraction remains speculative. Other complexes bearing the 6-[2-BR_2-phenyl]pyrid-2-yl motif like **Zr-1** can in principle also be capable of promoting the ROMP of NBE but might be too unstable in the presence of E to allow for any ROMP-derived poly(NBE) structures under such conditions. While the fundamentals for a switch from VIP to ROMP have now been clarified, the low polymerization activity remains a challenge. The highly constrained geometry of the **Zr-2**, the resulting low propensity to undergo β-hydride elimination together with the possibility to undergo cross-metathesis with E accounts for a very low productivity. One key to higher activities seems therefore the suppression of cross-metathesis of the propagation alkylidenes with E. Progress in this issue will be reported in due course.

Experimental

All manipulations were conducted by using standard Schlenk or dry box techniques under an atmosphere of Argon or nitrogen unless specified otherwise. Deuterated solvents for NMR were freeze–pump–thaw degassed and stored inside a glove box. Benzene-d_6, toluene-d_8 and tetrahydrofuran-d_8 were dried and distilled from sodium/benzophenone; CD_2Cl_2 and $CDCl_3$ were dried and distilled from P_2O_5; $C_2D_2Cl_4$ was distilled from calcium hydride. Regular solvents, *i.e.* diethyl ether, toluene, THF, *n*-pentane, CH_2Cl_2 were dried and deoxygenated by sparging with N_2, followed by passing through a triple-column solvent purification system (MBraun, Garching, Germany). Commercially available reagents for synthesis were used without further purification. Celite was dried *in vacuo* at 180 °C for two days prior to use. Methylalumoxane (MAO, 10 wt% solution in toluene) was purchased from Sigma-Aldrich. The toluene was removed and the residue was dried *in vacuo* at 80 °C overnight to remove any free $AlMe_3$ and stored inside a glove box. Ethylene gas was purified by passing through columns filled with Cu-catalyst (BASF R3-11G) and 3 Å molecular sieves before use. All homopolymerization reactions of NBE were carried out in Schlenk tubes under an inert atmosphere. All copolymerizations of ethylene with NBE were performed in a Büchi–Uster pressure reactor equipped with a Huber thermostat. The feed of ethylene was kept constant and ethylene consumption was monitored by a Büchi pressflow bpc 6010 flow controller.

NMR data were recorded at 400 MHz for ^{1}H and 100 MHz for ^{13}C on a Bruker Avance III 400 spectrometer at 25 °C unless noted otherwise and reported in ppm relative to tetramethylsilane (TMS). All NMR data of the homo-/copolymers were measured at 100 °C except where noted. FTIR spectra were measured on a Perkin-Elmer 881 spectrometer with ATR technology.

Molecular weights and molecular weight distributions were measured by high-temperature gel permeation chromatography (HT-GPC) on an Agilent PL-GPC 220 system equipped with three consecutive PLgel 5 μm MIXED-C 300 × 7.5 mm columns in 1,2,4-trichlorobenzene at 160 °C. The flow rate was set to 1 mL min^{-1}. The GPC system was calibrated with narrow polystyrene standards in the range of 162–6 035 000 g mol^{-1} (Easi Vial-red, yellow and green, Fig. S45†), which were all purchased from Polymer Labs. DSC data were recorded by heating under a nitrogen atmosphere on a Perkin–Elmer DSC7 differential scanning calorimeter.

2-Isopropylphenylboronic acid

To a solution of 1-bromo-2-isopropylbenzene (19.9 g, 0.10 mol) in 200 mL of THF cooled to −78 °C was added *n*-BuLi (66 mL, 1.6 M in hexane, 0.11 mol) and the resulting solution was stirred for another 15 minutes at −78 °C. A solution of tris(2-propyl)borate (62 mL, 0.27 mol) in 60 mL of THF was added drop wise. Afterwards, the resulting mixture was stirred for a further hour at −78 °C and then allowed to the room temperature for another 1 h. The system was quenched with aqueous HCl and extracted with ethyl acetate. After removal of the solvents, the crude was recrystallized from CH_2Cl_2. Yield: 9.88 g (60.2%). ^{1}H NMR (DMSO-d_6): δ = 0.45 (d, 6H, $^3J_{HH}$ = 6.9 Hz, isopropyl), 1.35 (s, 2H, $B(OH)_2$), 2.50 (m, 1H, isopropyl), 6.37 (t, 1H, $^3J_{HH}$ = 7.0 Hz, H–C_5 of phenyl), 6.51 (1H, d, $^3J_{HH}$ = 7.6 Hz, H–C_3 of phenyl), 6.54 (t, 1H, $^3J_{HH}$ = 7.4 Hz, H–C_4 of phenyl) 6.57 (d, 1H, $^3J_{HH}$ = 7.2 Hz, H–C_6 of phenyl). ^{13}C NMR (DMSO-d_6): δ = 24.4 (CH_3 of isopropyl), 32.6 (*C*H of isopropyl), 124.1 ($C_{3,5}$ of phenyl), 124.6 (C_4 of phenyl), 128.6 (C_6 of phenyl), 132.2(C_1 of phenyl), 151.5 (C_2 of phenyl).

6-(2-Isopropylphenyl)pyridin-2-amine

A solution of 2-amino-6-bromopyridine (8.65 g, 0.05 mol) and $Pd(PPh_3)_4$ (0.30 g, 0.26 mmol) in toluene (240 mL) was stirred for 10 minutes. 2-Isopropylphenylboronic acid (8.20 g, 0.05 mol), ethanol (90 mL), sodium carbonate (10.6 g, 0.10 mol) and water (120 mL) were added successively. The degassed mixture was heated at reflux overnight, then cooled to room temperature and the aqueous phase was extracted with ethyl acetate. The combined extracts were dried over magnesium sulphate and concentrated *in vacuo* to give a solid. This solid was subjected to chromatography on silica gel using the mixture (ethyl acetate–CH_2Cl_2–pentane = 1 : 1 : 5, 2 or 3 drops of triethylamine per 1000 mL of solvents) as eluent. Yield: 10.3 g (97.2%). ^{1}H NMR ($CDCl_3$): δ = 1.19 (d, 6H, $^3J_{HH}$ = 6.9 Hz, isopropyl), 3.20 (m, 1H, isopropyl), 4.52 (s, 2H, NH_2), 6.45 (d, 1H, $^3J_{HH}$ = 8.2 Hz, PyH), 6.70 (d, 1H, $^3J_{HH}$ = 7.3 Hz, PyH), 7.22 (m, 1H, PyH), 7.27 (dd, 1H, $^3J_{HH}$ = 3.3, 9.9 Hz, ArH), 7.35 (m, 1H, ArH), 7.39 (d, 1H, $^3J_{HH}$ = 7.3 Hz, ArH), 7.48 (t, 1H, $^3J_{HH}$ = 7.8 Hz, ArH). ^{13}C NMR (benzene-d_6): δ = 24.3, 29.4, 106.6, 114.5, 125.5, 125.7, 128.4, 129.4, 137.8, 140.2, 146.5, 157.9, 158.9. FT-IR (ATR mode, cm^{-1}): $\bar{\nu}$ = 3461 (m), 3292 (m), 3127 (s), 2962 (m), 1629 (s), 1591 (w), 1567 (w), 1461 (s), 1354 (m), 1262 (m), 1052 (w), 985 (m), 800 (m), 757 (s). MS (ESI) [*m*/*z*] calcd for $C_{14}H_{16}N_2$: 212.1, found 213.1 ($[M + H]^+$, 75%), 235.1 ($[M + Na]^+$, 25%).

Compound 3

To a solution of **1** (1.9 g, 8.0 mmol) in pentane–diethyl ether (10 : 1) was added *n*-butyllithium (1.6 M in hexane, 5.0 mL, 8.0 mmol) at −35 °C and the mixture was warmed to room temperature and stirred for 2 h. The precipitate was filtered and washed with cold pentane–diethyl ether (10 : 1) and dried *in vacuo* to give a light-yellow solid. Yield: 2.2 g (86.4%).

The suspension of **1**·Li(Et_2O) (1.59 g, 5.0 mmol) in diethyl ether (50 mL) at −35 °C was added to a solution of **2** (1.29 g, 5.0 mmol) in diethyl ether (13 mL). After the mixture was stirred overnight at room temperature, LiCl was filtered off and diethyl ether was removed *in vacuo* to give a white crude solid, which was recrystallized from CH_2Cl_2 and pentane to yield white crystals. Yield: 1.9 g (82.5%). ^{1}H NMR (C_6D_6): δ = 7.81–7.76 (m, 1H), 7.73 (dd, *J* = 6.9, 1.1 Hz, 2H), 7.61 (dt, *J* = 7.7, 0.8 Hz, 1H), 7.47–7.38 (m, 3H), 7.30–7.19 (m, 5H), 6.98 (t, *J* = 7.9 Hz, 1H), 6.80 (dd, *J* = 7.6, 0.9 Hz, 1H), 6.02 (dd, *J* = 8.3, 0.9 Hz, 1H), 5.69 (s, 1H), 3.82 (s, 1H), 1.26 (dq, *J* = 15.4, 7.7 Hz, 2H), 1.03–0.88 (m, 2H), 0.74 (t, *J* = 7.6 Hz, 6H), 0.00–0.15 (m, 6H). ^{1}H NMR (CD_2Cl_2): δ = 7.89 (d, *J* = 7.6 Hz, 2H), 7.74–7.70 (m, 1H), 7.65 (t, *J* = 7.9 Hz, 1H), 7.57 (dd, *J* = 7.5, 0.9 Hz, 2H), 7.48–7.44 (m, 1H), 7.43–7.37 (m, 2H), 7.37–7.29 (m, 3H), 7.24 (ddd, *J* = 15.2, 7.5, 1.0 Hz, 2H), 6.44 (dd, *J* = 8.3, 0.8 Hz, 1H), 5.43 (s, 1H), 4.25 (s, 1H), 0.71 (dq, *J* = 15.4, 7.7 Hz, 2H), 0.50 (tt, *J* = 14.5, 7.4 Hz, 2H), 0.31–0.22 (m, 12H). ^{13}C NMR (C_6D_6): δ = 163.6, 158.1, 155.9, 143.7, 141.4, 140.2, 137.7, 130.4, 129.5, 126.9, 126.6, 125.6, 124.7, 121.3, 120.7, 107.8, 106.3, 41.9, 15.1, 10.4, −3.8. ESI-MS: *m*/*z* calcd for $C_{30}H_{33}BN_2Si$: 460.25; found: 461.26 $[M + H]^+$. Elemental analysis calcd (%) for $C_{30}H_{33}BN_2Si$: C 78.25, H 7.22, N 6.08; found: C 78.03, H 7.26, N 6.04. FTIR (ATR mode): 3378 (s), 2940 (m), 2857 (m), 1622 (s), 1571 (vs), 1486 (vs), 1447 (s), 1377 (s), 1255 (s), 1171(s), 833 (vs), 801 (vs), 734 (vs).

Compound 4

To a solution of **3** (1.125 g, 2.44 mmol) in 15 mL toluene at −35 °C were added 2 equivalents of *n*-BuLi (1.6 M in hexane, 3.05 mL, 4.88 mmol). After the solution was stirred 2 h at room temperature, the solvent was removed *in vacuo* and the resulting orange residue was recrystallized from THF and pentane at −35 °C to give yellow crystals. Yield: 1.63 g (80.7%). ^{1}H NMR (C_6D_6): δ = 8.27–8.16 (m, 4H), 7.82 (t, *J* = 6.5 Hz, 2H), 7.48–7.40 (m, 1H), 7.37–7.27 (m, 4H), 7.09–7.01 (m, 2H), 6.93 (dd, *J* = 8.6, 0.8 Hz, 1H), 6.83 (dd, *J* = 7.0, 0.9 Hz, 1H), 2.95 (q, *J* = 6.5 Hz, 20H, THF), 1.23–1.08 (m, 20H, THF), 1.07–0.92 (m, 16H). ^{13}C NMR (C_6D_6): δ = 163.8, 157.8, 140.6, 140.3, 137.0, 128.9, 125.0, 124.8, 122.9, 120.6, 120.1, 120.0, 115.7, 114.6, 98.6, 81.5, 67.6 (s, C–O, THF), 25.3 (s, C–O, THF), 13.2, 11.1, 3.4. Elemental analysis calcd (%) for $C_{50}H_{71}BN_2O_5SiLi_2$(THF): C 71.67, H 8.80, N 3.10; found: C 71.64, H 8.48, N 3.46.

Complex Zr-1

A solution of **4** (1.43 g, 1.58 mmol) in toluene (15 mL) at −35 °C was added to a solution of $ZrCl_4$·2THF (596 mg, 1.58 mmol) in THF and the resulting orange–red mixture was stirred at room temperature for 36 h. LiCl was filtered off and all solvents was removed *in vacuo*. The resulting red residue was dissolved in toluene (10 mL) and stirred for 15 min, followed by the removal of any insoluble solid *via* filtration through celite. After the removal of the solvent, the red solid was recrystallized from CH_2Cl_2 and pentane at −35 °C. Yield: 220 mg (18.2%). ^{1}H NMR (CD_2Cl_2): δ = 8.10 (d, *J* = 7.6 Hz, 2H), 8.07–7.95 (m, 3H), 7.84 (d, *J* = 7.7 Hz, 1H), 7.67 (dd, *J* = 7.7, 0.9 Hz, 1H), 7.55 (dt, *J* = 15.0, 4.1 Hz, 3H), 7.44–7.33 (m, 3H), 7.28 (td, *J* = 7.5, 1.2 Hz, 1H), 7.09 (dd, *J* = 8.1, 0.8 Hz, 1H), 3.00 (s, 4H, THF), 1.49 (t, *J* = 6.6 Hz, 4H, THF), 0.77 (d, *J* = 59.3 Hz, 10H), 0.47 (dd, *J* = 8.3, 6.4 Hz, 6H). ^{1}H NMR (C_6D_6): δ = 8.24 (d, *J* = 7.7 Hz, 2H), 7.89 (d, *J* = 7.2 Hz, 1H), 7.78 (d, *J* = 7.6 Hz, 2H), 7.66 (d, *J* = 7.7 Hz, 1H), 7.50–7.37 (m, 3H), 7.27 (td, *J* = 7.6, 1.1 Hz, 1H), 7.19 (ddd, *J* = 7.8, 4.2, 2.3 Hz, 3H), 7.06 (dd, *J* = 7.7, 1.0 Hz, 1H), 6.96 (dd, *J* = 8.0, 0.8 Hz, 1H), 2.55 (s, 4H), 1.53 (s, 4H), 1.05 (s, 6H), 0.60 (s, 10H). ^{13}C NMR (C_6D_6): δ = 165.2, 162.5, 159.3, 140.3, 137.1, 130.2, 129.7, 126.8, 125.4, 123.7, 122.0, 121.4, 120.3, 116.3, 111.2, 99.4, 76.4 (THF), 25.1 (THF), 11.9, 1.4, −0.1. ^{13}C NMR (CD_2Cl_2): δ = 162.5, 158.8, 140.9, 137.5, 137.2, 129.7, 129.3, 127.2, 125.3, 124.1, 121.8, 121.3, 120.7, 117.0, 111.4, 99.7, 75.9 (THF), 25.9 (THF), 11.2, 4.1, 4.0, −0.1. Elemental analysis calcd (%) for $C_{34}H_{39}BCl_2N_2OSiZr$ $(THF)_{1/4}(CH_2Cl_2)_{1/4}$: C 57.84, H 5.71, N 3.83; found: C 57.87, H 5.65, N 3.94. Crystals suitable for single-crystal X-ray analysis were obtained by recrystallization from CH_2Cl_2–pentane.

Complex Hf-1

A solution of **4** (400 mg, 0.442 mmol) in toluene (15 mL) at −35 °C was added to a suspension of $HfCl_4$·2THF (205 mg,

0.442 mmol) in toluene; then the yellow mixture was stirred at room temperature for 24 h. Lithium chloride was filtered off and the solvent was removed *in vacuo*. The resulting red residue was dissolved in toluene and any insoluble solid was filtered off through a pad of celite. After the removal of the solvent, the red solid was recrystallized from toluene and pentane at −35 °C. Yield: 35 mg (9.2%). ^{1}H NMR (C_6D_6): δ = 8.19 (d, J = 48.0 Hz, 2H), 7.92 (d, J = 7.2 Hz, 1H), 7.83 (d, J = 7.4 Hz, 2H), 7.68 (d, J = 7.7 Hz, 1H), 7.48–7.39 (m, 3H), 7.28 (td, J = 7.5, 1.2 Hz, 2H), 7.22 (t, J = 7.8 Hz, 1H), 7.06 (dd, J = 7.7, 1.0 Hz, 1H), 7.04–7.00 (m, 1H), 2.50 (d, 3H), 1.64 (d, 2H), 1.03 (s, 6H), 0.54 (s, 4H), 0.20 (s, 4H). ^{13}C NMR (C_6D_6): δ = 165.4, 162.5, 159.3, 145.6, 140.1, 139.3, 138.0, 137.2, 136.3, 130.2, 129.6, 129.3, 128.1, 126.8, 125.3, 124.2, 123.6, 123.0, 121.4, 120.7, 119.1, 117.9, 111.3, 96.1, 77.3, 25.2, 10.4, 2.6, 1.4. Elemental analysis calcd (%) for $C_{34}H_{39}BCl_2N_2OSiHf$ $(THF)_{1/2}$: C 52.99, H 5.31, N 3.43; found: C 53.07, H 5.35, N 3.53. Crystals suitable for single-crystal X-ray analysis were grown from toluene–pentane.

Compound 5

To a solution of 2-(2-bromophenyl)-6-(2,2,5,5-tetramethyl-1,2,5-azadisilolidin-1-yl)pyridine (2.0, 5.1 mmol) in diethyl ether was slowly added a solution of *n*-butyl lithium (2.5 M, 2.45 mL, 6.1 mmol) in hexane at −78 °C and the mixture was stirred for 1.5 h at this temperature. A solution of dimesitylboron fluoride (2.06 g, 7.66 mmol) in THF (10 mL) was added and the mixture was stirred for a further hour at −78 °C, then gradually warmed to room temperature and stirred overnight. Ice water was added to hydrolyze the protecting group and the solution was stirred for 30 min. The mixture was diluted with ethyl acetate, washed with water and brine and dried over $MgSO_4$. After removal of the solvent, the residue was subjected to chromatography on silica gel eluting with hexane–ethyl acetate (9 : 1) to yield the target product.[31,32] Yield: 0.97 g (45.5%). ^{1}H NMR (THF-d_8): δ = 7.81–7.72 (m, 1H), 7.71–7.62 (m, 2H), 7.33 (dd, J = 7.5, 1.1 Hz, 1H), 7.13–6.99 (m, 2H), 6.56 (s, 4H), 6.42 (dd, J = 8.3, 1.1 Hz, 1H), 6.28 (s, 2H, NH_2), 2.10 (s, 6H), 2.00–1.76 (m, 12H). ^{13}C NMR (THF-d_8): δ = 159.2, 158.2, 144.1, 141.8, 136.8, 134.0, 131.0, 129.5, 125.2, 122.2, 110.1, 105.4, 67.2, 25.1, 20.6. ESI-MS: m/z calcd for $C_{29}H_{31}BN_2$: 418.26; found: 419.26 $[M + H]^+$. FTIR (ATR mode): 3446 (m), 3348 (s), 2907 (m), 1633 (s), 1603 (vs), 1566 (s), 1493 (s), 1444 (s), 846 (m), 753 (vs), 729 (m), 702 (s).

Compound 6

To a solution of **5** (900 mg, 2.15 mmol) in 25 mL of THF at −35 °C was added *n*-BuLi (1.6 M in hexane, 1.34 mL, 2.15 mmol). After the solution was stirred 3 h at room temperature, the solvent was removed *in vacuo* and the resulting orange residue was washed twice with pentane to give a yellow solid, which was used without any further purification. Due to its sensitivity and instability, only the ^{1}H NMR spectrum was recorded. ^{1}H NMR (C_6D_6): δ = 8.04 (d, J = 7.3 Hz, 1H), 7.67 (d, J = 7.4 Hz, 1H), 7.20 (dd, J = 12.1, 5.9 Hz, 1H), 7.15–7.10 (m, 1H), 7.04 (t, J = 7.7 Hz, 1H), 6.71 (t, J = 23.4 Hz, 5H), 6.07 (d, J = 8.4 Hz, 1H), 4.79 (s, 1H), 3.20 (d, J = 6.1 Hz, 8H), 2.16 (s, 18H), 1.35–1.15 (m, 8H).

Compound 7

To a solution of **6** (1.977 g, 3.47 mmol) in diethyl ether (50 mL) at −35 °C was added a solution of chlorodimethyl (2,3,4,5-tetramethylcyclopenta-2,4-dienyl)silane (768 μL, 3.47 mmol) in diethyl ether (5 mL). After the mixture was stirred overnight at room temperature, lithium chloride was filtered off and diethyl ether was removed *in vacuo* to yield a pink crude solid, which was subsequently recrystallized from diethyl ether and pentane to give a white solid. Yield: 1.70 g (82.1%). ^{1}H NMR (C_6D_6): δ = 8.08 (d, J = 7.7 Hz, 1H), 7.54 (d, J = 7.5 Hz, 1H), 7.13 (dd, J = 7.5, 1.1 Hz, 1H), 7.07–6.97 (m, 2H), 6.85 (dd, J = 7.6, 1.0 Hz, 1H), 6.75 (s, 4H), 6.41 (s, 1H, NH), 6.26 (dd, J = 8.3, 1.0 Hz, 1H), 2.89 (s, 1H), 2.16 (d, J = 7.3 Hz, 18H), 1.68 (s, 6H), 1.52 (s, 6H), −0.06 (s, 6H). ^{13}C NMR (C_6D_6): δ = 159.6, 159.2, 142.2, 140.6, 137.9, 137.2, 135.9, 134.5, 131.8, 131.1, 130.7, 129.5, 128.1, 125.2, 122.2, 110.0, 106.0, 54.2, 25.3, 20.8, 13.8, 11.2, −3.6. Elemental analysis calcd (%) for $C_{40}H_{49}BN_2Si$: C 80.51, H 8.28, N 4.69; found C 80.41, H 8.43, N 4.43. ESI-MS: m/z calcd for $C_{40}H_{49}BN_2Si$: 596.38; found. 619.38 $[M + Na]^+$. FTIR (ATR mode): 3291 (m), 2913 (m), 1624 (m), 1560 (s), 1490 (vs), 1438 (s), 845 (s), 820 (vs), 756 (vs), 699 (s).

Complex Zr-2

To a solution of **7** (1.0 g, 1.676 mmol) in toluene (10 mL) at −35 °C were added 2 equivalents of *n*-BuLi (1.6 M in hexane, 2.1 mL, 3.35 mmol). The solution was allowed to warm to room temperature and stirred for 2 h, then re-chilled to −35 °C and finally added to a solution of $ZrCl_4$·2THF (632 mg, 1.676 mmol) in toluene (10 mL). The resulting brown mixture was stirred at room temperature for 36 h. LiCl was filtered off and the solvent was removed *in vacuo.* The resulting earth-yellow residue was dissolved in toluene and filtered off insoluble solid. After the removal of the solvent, the solid was recrystallized from toluene and pentane at −35 °C. Yield: 412 mg (32.5%). ^{1}H NMR (C_6D_6): δ = 9.19 (dd, J = 7.8, 0.7 Hz, 1H), 7.58 (dd, J = 7.5, 0.9 Hz, 1H), 7.50 (td, J = 7.6, 1.4 Hz, 1H), 7.10 (td, J = 7.5, 1.2 Hz, 1H), 6.82–6.72 (m, 2H), 6.64 (s, 4H), 5.34 (dd, J = 7.5, 1.4 Hz, 1H), 2.16 (s, 12H), 2.09 (t, J = 4.7 Hz, 18H), 0.41 (s, 6H). ^{13}C NMR (C_6D_6): δ = 162.7, 157.7, 148.7, 143.9, 143.5, 141.4, 139.3, 138.6, 135.9, 131.8, 131.6, 131.3, 130.5, 129.0, 128.8, 120.2, 106.7, 102.6, 24.2, 21.3, 14.5, 11.9, 2.8. Elemental analysis calcd (%) for $C_{40}H_{47}BCl_2N_2OSiZr$: C 63.48, H 6.26, N 3.70; found C 63.13, H 6.42, N 3.62. Crystals suitable for single-crystal X-ray analysis were grown from toluene–pentane.

Compound 8

To a solution of 6-(2-isopropylphenyl)pyridin-2-amine (1.06 g, 5.0 mmol) in diethyl ether (25 mL) was added a butyllithium solution (1.6 M in hexane, 3.12 mL, 5.0 mmol) at −35 °C. After 1 min, a precipitate formed and the mixture was allowed to warm to room temperature and stirred for another 10 minutes. The suspension was cooled to −35 °C again and a solution of **2** (1.29 g, 5.00 mmol) in diethyl ether (20 mL) was added. The

mixture was warmed to room temperature and stirred for another 2 h. The precipitate was filtered off and the resulting filtrate was dried *in vacuo.* The residue was recrystallized from diethyl ether and pentane to obtain a green solid. Yield: 1.98 g (91.1%). ^{1}H NMR ($CDCl_3$): δ = 7.85 (d, J = 7.5 Hz, 6H), 7.52 (t, J = 7.8 Hz, 3H), 7.43 (d, J = 7.5 Hz, 6H), 7.41–7.36 (m, 4H), 7.36–7.30 (m, 11H), 7.26–7.18 (m, 8H), 6.74 (d, J = 7.4 Hz, 3H), 6.50 (d, J = 8.2 Hz, 3H), 4.56 (s, 3H), 4.19 (s, 3H), 3.42 (dq, J = 13.7, 6.8 Hz, 3H), 1.17 (d, J = 6.9 Hz, 18H), 0.02–0.05 (m, 18H). ^{1}H NMR (C_6D_6): δ = 7.77 (d, J = 7.6 Hz, 6H), 7.48–7.39 (m, 9H), 7.29–7.22 (m, 10H), 7.08 (td, J = 7.4, 1.4 Hz, 3H), 6.65 (dd, J = 7.4, 0.8 Hz, 3H), 5.96 (dd, J = 8.2, 0.8 Hz, 3H), 4.78 (s, 3H), 3.71–3.53 (m, 6H), 1.14 (d, J = 6.9 Hz, 18H), −0.01–0.09 (m, 17H). ^{13}C NMR ($CDCl_3$): δ = 159.2, 159.1, 146.4, 145.1, 140.8, 140.7, 137.8, 129.7, 128.2, 126.2, 125.5, 125.4, 124.5, 120.0, 114.6, 108.1, 77.2, 42.0, 29.2, 24.3, −3.5. ESI-MS: m/z calcd for $C_{29}H_{30}N_2Si$: 434.22; found 435.22 $[M + H]^+$. FTIR (ATR mode): 3404 (m), 2957 (m), 1588 (s), 1571 (s), 1460 (s), 1493 (s), 1371 (s), 1294 (s), 1036 (s), 855 (s), 801 (vs), 740 (vs).

Compound 9

To a solution of **8** (1.5 g, 3.45 mmol) in toluene (7 mL) at −35 °C were added 2 equivalents of *n*-BuLi (1.6 M in hexane, 4.31 mL, 6.90 mmol). The solution was stirred for 2 h at room temperature, followed by the removal of the solvent. The resulting orange residue was recrystallized from THF and pentane at −35 °C to give yellow crystals, which turned out to be unstable even at low temperature. Yield: 1.83 g (72.5%). ^{1}H NMR (THF-d_8): δ = 7.82 (d, J = 7.5 Hz, 2H), 7.70 (d, J = 8.1 Hz, 2H), 7.11 (dd, J = 16.0, 7.6 Hz, 3H), 6.98 (t, J = 7.4 Hz, 1H), 6.76 (d, J = 24.1 Hz, 3H), 6.39 (s, 2H), 6.26 (d, J = 8.3 Hz, 1H), 5.67 (d, J = 6.2 Hz, 1H), 3.55 (d, J = 4.9 Hz, 3H), 3.44 (s, 1H), 1.69 (s, 4H), 1.09 (d, J = 6.9 Hz, 6H), 0.48 (s, 6H).

Complex Zr-3

A solution of **9** (1.24 g, 1.694 mmol) in toluene (5 mL) at −35 °C was added to a solution of $ZrCl_4$·2THF (639 mg, 1.694 mmol) in THF (10 mL); then the mixture was stirred at room temperature for 36 h. Lithium chloride was filtered off and all solvents were removed *in vacuo*. The resulting red residue was dissolved in CH_2Cl_2 and filtered through a pad of celite. After the removal of the solvent and recrystallization from CH_2Cl_2 and pentane at −35 °C, an orange solid was obtained. Yield: 283 mg (17.5%). ^{1}H NMR (C_6D_6): δ = 8.05 (d, J = 8.1 Hz, 4H), 7.85–7.78 (m, 6H), 7.30 (ddd, J = 8.2, 7.0, 1.2 Hz, 4H), 7.21 (ddd, J = 8.0, 7.0, 1.0 Hz, 5H), 7.06–7.03 (m, 3H), 6.98 (dt, J = 9.9, 5.0 Hz, 2H), 6.44 (dd, J = 7.6, 0.9 Hz, 2H), 5.82 (dd, J = 8.2, 0.9 Hz, 2H), 3.07 (dt, J = 13.6, 6.8 Hz, 2H), 2.94 (s, 8H), 1.19 (d, J = 6.8 Hz, 12H), 0.88 (td, J = 6.7, 3.0 Hz, 9H), 0.64 (d, J = 3.4 Hz, 12H). ^{13}C NMR (C_6D_6): δ = 165.7, 156.4, 146.8, 141.9, 140.8, 137.4, 134.6, 130.4, 129.4, 128.1, 126.5, 125.8, 125.4, 124.9, 123.3, 121.0, 117.1, 108.2, 83.1, 74.3, 30.4, 25.2, 24.7, 1.1. Elemental analysis calcd (%) for $C_{36}H_{40}BCl_2N_2OSiZr$ (CH_2Cl_2) $(toluene)_{1/4}$: C 61.00, H 5.73, N 3.98; found C 61.25, H 5.85, N 4.31.

Variable-temperature ^{1}H and ^{11}B NMR

Manipulations were carried out inside a glove box under a nitrogen atmosphere. Catalyst : MAO : NBE = 1 : 30 : 10, [catalyst] = 0.08 mol L^{-1}. MAO or MAO/NBE were dissolved in toluene-d_8 and kept in an NMR tube, after cooling at −37 °C for 2 h, a chilled solution of the catalyst in toluene-d_8 was added to the NMR tube. The total volume of the solution was ~ 0.6 mL. The NMR tube was chilled in liquid nitrogen prior to ^{1}H and ^{11}B NMR measurements.

General procedure for NBE homopolymerization

All preparations were carried out inside a glove box. Defined amounts of NBE and MAO were dissolved in toluene (45 mL) in a Schlenk tube. The mixture was stirred for 5 min prior to the addition of a defined amount of catalyst in toluene (5 mL) and heated to the desired temperature. The reaction was quenched after 1 h by the addition of methanol (10 mL). The resulting mixture was poured into a solution of acidic methanol (500 mL of methanol containing 10 mL of concentrated HCl). The polymer was collected by filtration and washed with methanol (3 × 100 mL), then dried *in vacuo* at 50 °C for 2 days.

General procedure for E-NBE copolymerization

Samples were prepared inside a glove box. Polymerization reactions were carried out in a Büchi glass reactor (500 mL), which was dried at 120 °C *in vacuo* for 2 h, cooled to 30 °C and purged with Ar gas prior to use. A mixture of monomer and MAO in toluene (*ca*. 245 mL) and a solution of the catalyst in toluene (*ca*. 5 mL) were quickly introduced into the reactor and stirred (300 rpm) at 30 °C. Ethylene gas was introduced once the mixture had reached the desired temperature. The reaction was quenched after 1 h by the addition of methanol (10 mL). The resulting mixture was poured into a solution of acidic methanol (500 mL of methanol containing 10 mL of concentrated HCl). The polymer was collected by filtration and washed with methanol (3 × 100 mL), then dried *in vacuo* at 50 °C for 2 days.

Acknowledgements

Financial support by the Deutsche Forschungsgemeinschaft (DFG, grant-nr: 2174/14-1) is gratefully acknowledged.

Notes and references

1 M. R. Buchmeiser, *Curr. Org. Chem.*, 2013, **17**, 2764–2775.
2 M. R. Buchmeiser, S. Camadanli, D. Wang, Y. Zou, U. Decker, C. Kühnel and I. Reinhardt, *Angew. Chem., Int. Ed.*, 2011, **123**, 3628–3633.
3 Y. Zou, D. Wang, K. Wurst, C. Kühnel, I. Reinhardt, U. Decker, V. Gurram, S. Camadanli and M. R. Buchmeiser, *Chem. – Eur. J.*, 2011, **17**, 13832–13846.
4 B. P. Carrow and K. Nozaki, *Macromolecules*, 2014, **47**, 2541–2555.

5 T. C. M. Chung, *Macromolecules*, 2013, **46**, 6671–6698.
6 M. Ciftci, P. Batat, A. L. Demirel, G. Xu, M. Buchmeiser and Y. Yagci, *Macromolecules*, 2013, **46**, 6395–6401.
7 J.-Y. Dong and Y. Hu, *Coord. Chem. Rev.*, 2006, **250**, 47–65.
8 N. M. Franssen, J. N. Reek and B. de Bruin, *Chem. Soc. Rev.*, 2013, **42**, 5809–5832.
9 G. Xu, D. Wang and M. R. Buchmeiser, *Macromol. Rapid Commun.*, 2012, **33**, 75–79.
10 Z. Jian, P. Wucher and S. Mecking, *Organometallics*, 2014, **33**, 2879–2888.
11 H. Leicht, I. Göttker-Schnetmann and S. Mecking, *Angew. Chem., Int. Ed.*, 2013, **125**, 4055–4058.
12 K. E. Allen, J. Campos, O. Daugulis and M. Brookhart, *ACS Catal.*, 2015, **5**, 456–464.
13 A. C. Gottfried and M. Brookhart, *Macromolecules*, 2003, **36**, 3085–3100.
14 S. D. Ittel, L. K. Johnson and M. Brookhart, *Chem. Rev.*, 2000, **100**, 1169–1203.
15 G. V. Narayana, G. Xu, D. Wang, W. Frey and M. R. Buchmeiser, *ChemPlusChem*, 2014, **79**, 151–162.
16 G. Xu, G. V. Narayana, M. Speiser, D. Wang, Y. Zou and M. R. Buchmeiser, *Macromol. Chem. Phys.*, 2014, **215**, 893–899.
17 H. G. Alt and E. Samuel, *Chem. Soc. Rev.*, 1998, **27**, 323–329.
18 G. W. Coates, *Chem. Rev.*, 2000, **100**, 1223–1252.
19 T. Senda, H. Hanaoka, S. Nakahara, Y. Oda, H. Tsurugi and K. Mashima, *Macromolecules*, 2010, **43**, 2299–2306.
20 S. Gentil, M. Dietz, N. Pirio, P. Meunier, J. C. Gallucci, F. Gallou and L. A. Paquette, *Organometallics*, 2002, **21**, 5162–5166.
21 A. A. H. Van Der Zeijden, C. Mattheis and R. Fröhlich, *Chem. Ber.*, 1997, **130**, 1231–1234.
22 J. A. Ewen, *Macromol. Symp.*, 1995, **89**, 181–196.
23 J. Okuda, F. J. Schattenmann, S. Wocadlo and W. Massa, *Organometallics*, 1995, **14**, 789–795.
24 L. J. Irwin, J. H. Reibenspies and S. A. Miller, *J. Am. Chem. Soc.*, 2004, **126**, 16716–16717.
25 S. A. Miller and J. E. Bercaw, *Organometallics*, 2006, **25**, 3576–3592.
26 E. Kirillov, L. Toupet, C. W. Lehmann, A. Razavi and J.-F. Carpentier, *Organometallics*, 2003, **22**, 4467–4479.
27 M. A. Schmid, H. G. Alt and W. Milius, *J. Organomet. Chem.*, 1995, **501**, 101–106.
28 *Stereoselective Polymerization With Single-Site Catalysts*, ed. C. J. Price, L. J. Irwin, D. A. Aubry and S. A. Miller, CRC Press, Boca Raton, FL, 2008.
29 R. Tanaka, I. Kamei, Z. Cai, Y. Nakayama and T. Shiono, *J. Polym. Sci., Part A: Polym. Chem.*, 2015, **53**, 685–691.
30 L. J. Irwin, J. H. Reibenspies and S. A. Miller, *Polyhedron*, 2005, **24**, 1314–1324.
31 H. Amarne, C. Baik, S. K. Murphy and S. Wang, *Chem. – Eur. J.*, 2010, **16**, 4750–4761.
32 Y.-L. Rao, H. Amarne, J.-S. Lu and S. Wang, *Dalton Trans.*, 2013, **42**, 638–644.
33 S. Hermanek, *Chem. Rev.*, 1992, **92**, 325–362.
34 F. Teixidor, M. A. Flores, C. Viñas, R. Sillanpää and R. Kivekäs, *J. Am. Chem. Soc.*, 2000, **122**, 1963–1973.
35 Y.-L. Rao, H. Amarne, S.-B. Zhao, T. M. McCormick, S. Martić, Y. Sun, R.-Y. Wang and S. Wang, *J. Am. Chem. Soc.*, 2008, **130**, 12898–12900.
36 I. Tritto, L. Boggioni, C. Zampa and D. R. Ferro, *Macromolecules*, 2005, **38**, 9910–9919.
37 P. Sudhakar, *J. Polym. Sci., Part A: Polym. Chem.*, 2008, **46**, 444–452.
38 D. E. Babushkin, N. V. Semiloenova, V. N. Panchenko, A. P. Sobolov, V. A. Zakharov and E. P. Talsi, *Macromol. Chem. Phys.*, 1997, **198**, 3845–3854.
39 D. Cam and U. Giannini, *Makromol. Chem.*, 1992, **193**, 1049–1055.
40 W. Kaminsky and R. Steiger, *Polyhedron*, 1988, **7**, 2375–2381.
41 W. Kaminsky, *Macromol. Chem. Phys.*, 1996, **197**, 3907–3945.
42 J. Schwartz and K. I. Gell, *J. Organomet. Chem.*, 1980, **184**, C1–C2.
43 M. D. Fryzuk and S. S. H. Mao, *J. Am. Chem. Soc.*, 1993, **115**, 5336–5337.
44 M. D. Fryzuk, P. B. Duval, S. S. S. H. Mao, M. J. Zaworotko and L. R. MacGillivray, *J. Am. Chem. Soc.*, 1999, **121**, 2478–2487.
45 M. Kamitani, B. Pinter, C.-H. Chen, M. Pink and D. J. Mindiola, *Angew. Chem., Int. Ed.*, 2014, **126**, 11093–11095.
46 F. M. Hartner Jr., J. Schwartz and S. M. Clift, *J. Am. Chem. Soc.*, 1983, **105**, 640–641.

